

# Microstructural properties of thermal induced microcrystalline silicon carbide thin films deposited by HWCVD

**J Khoele, S Halindintwali, B A Julies and S Mkhwanazi**

Physics department, University of the Western Cape, Private Bag X17, Bellville 7535, South Africa

E-mail: 3075072@uwc.ac.za

**Abstract.** Amorphous Silicon carbide samples were prepared by Hot –Wire Chemical Vapor Deposition (HWCVD) at low temperature of the substrate. A gradual thermal annealing under vacuum induced a network rearrangement as shown by a change in the samples microstructure. The breaking of Si-H<sub>n</sub> and C-H<sub>n</sub> bonds, followed by hydrogen effusion, led all the available carbon atoms, originating mainly from C-H<sub>n</sub> groups to bond to the Si atoms originating mainly from the SiH<sub>n</sub> groups, and crystallize into SiC phase. The structural details are presented as studied by Fourier transform infrared spectroscopy (FTIR), transmission electron microscopy (TEM) and non contact atomic force microscopy (AFM).

## 1. Introduction

Crystalline silicon carbide (SiC) has a number of unique properties, like a wide band gap and high carrier mobility, which make the material an excellent candidate for various optoelectronic devices [1]. The wide optical band gap and the good electrical properties of SiC make the material particularly suitable for application as a window layer in silicon (Si) based solar cells. Because of the aptitude of the HWCVD to avail a high density of H radicals, crucial for microcrystalline growth, this deposition technique has been used by many groups to produce microcrystalline SiC films at low temperature of the substrate below 400 °C using monomethyl-silane (MMS) [1-4]. In this study we employed a SiH<sub>4</sub>/CH<sub>4</sub>/H<sub>2</sub> mixture to grow amorphous and nanocrystalline SiC by HWCVD at a low substrate temperature of 260°C. Thermal annealing of the films led to a fully crystalline SiC phase. We monitor these changes using FTIR and AFM analytical techniques.

## 2. Experimental details

The samples used in this study were deposited onto Corning glass and c-Si (100) substrates kept at 260 °C; a tungsten filament temperature of 2000 °C and a process pressure of 7.5 Pa were used in a commercial HWCVD system described elsewhere [5]. All samples were processed for a period of 40 minutes in order to achieve a thickness of less than 1µm. The thickness of the deposited layer was measured by a Veeco Dektak profilometer using the procedure described in [6]. Table 1 summarizes the deposition conditions. In order to study the re-organization and thermal crystallization, the samples were annealed at 700°C, 900°C and 1100°C for 60 minutes under vacuum conditions. FTIR absorption measurements were performed using a PerkinElmer Spectrum 100 spectrometer in the range between

400 and 4000  $\text{cm}^{-1}$ . The surface morphology of the films were investigated using a non-contact atomic force microscope (AFM) using a nanoscope instrument from Veeco Metrology Group. The TEM investigation was carried out by a TECNAI F20 (S)TEM instrument equipped with EDX (Energy Dispersive X-ray Spectroscopy) and EELS (Electron Energy Loss Spectroscopy).

**Table 1.** Deposition conditions of the samples used in this study.

Sample	F( $\text{SiH}_4$ ) (sccm)	F( $\text{CH}_4$ ) (sccm)	F( $\text{H}_2$ ) (sccm)	Thickness (nm)
S <sub>1</sub>	1.5	6	25.3	450
S <sub>2</sub>	1.5	6	5	580

### 3. Results

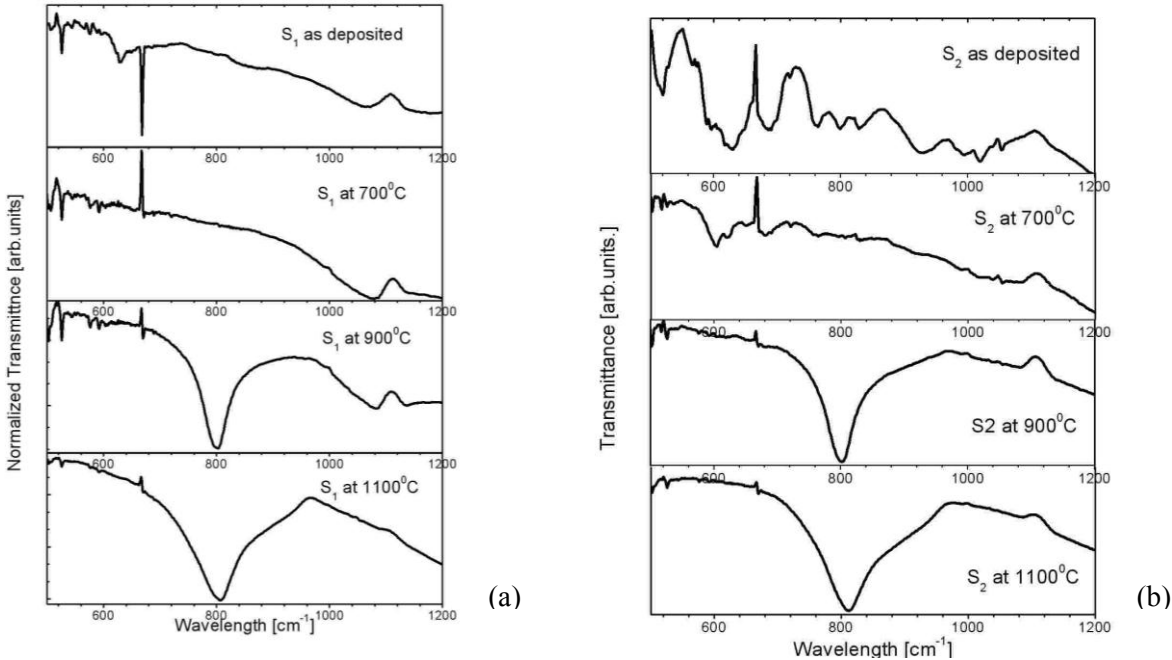
#### 3.1. Structural properties

Figure 1 shows the FTIR spectra of the samples as deposited on c-Si substrate and of those annealed under vacuum at different temperatures. The spectra of the as-deposited samples (top graphs figure 1(a) and figure 1(b)) show the characteristic features corresponding to  $(\text{SiH}_2)_n$  rocking / wagging at  $630 \text{ cm}^{-1}$  [7] in both samples S<sub>1</sub> and S<sub>2</sub>; this peak is more pronounced in S<sub>2</sub> that has been deposited with a much smaller partial flow rate of hydrogen in the gas mixture. Additional features of  $\text{SiH}_n$  are observed in the sample S<sub>2</sub> at  $\sim 830 \text{ cm}^{-1}$  and  $930 \text{ cm}^{-1}$  that have been assigned to  $\text{SiH}_2$  and  $\text{SiH}_3$  bending modes respectively [7]. Both spectra show also a sharp absorption peak due to SiC stretching bonds at  $670 \text{ cm}^{-1}$  and a broad band that extends from  $960 \text{ cm}^{-1}$  to  $1100 \text{ cm}^{-1}$  due to  $\text{CH}_n$  wagging/bending modes for the lower wavenumbers below  $1050 \text{ cm}^{-1}$  and to the asymmetric Si-O-Si stretching vibration or Si-O-C stretching modes for the higher wavenumbers above  $1050 \text{ cm}^{-1}$  [8-10]. Again additional absorption bands observed in the S<sub>2</sub> spectrum provides more insight into the SiC bonding: Well defined absorption bands were observed at  $765 \text{ cm}^{-1}$  and  $800 \text{ cm}^{-1}$ , they are assigned to  $\text{SiCH}_3$  stretching /wagging mode [11] and ordered Si-C crystalline phase [2] respectively. Moreover the absorption band from  $960 \text{ cm}^{-1}$  to  $1100 \text{ cm}^{-1}$  show much better distinguishable  $\text{CH}_n$  and oxidation corresponding components. The three subsequent graphs in fig. 1(a) and fig. 2(b) display the spectra of the samples annealed at  $700^\circ\text{C}$ ,  $900^\circ\text{C}$  and  $1100^\circ\text{C}$ . The main observation drawn from the spectra of the annealed samples at  $700^\circ\text{C}$  is a complete disappearance of the  $\text{SiH}_n$  related vibration bands in S<sub>1</sub> and a sharp decrease in their intensity in S<sub>2</sub>. The main feature observed on the spectra of the annealed samples at  $900^\circ\text{C}$  is a re-crystallization into SiC phase as shown by the emergence of the SiC signal at  $800 \text{ cm}^{-1}$  wavenumber but the  $\text{CH}_n$  component just above  $960^\circ\text{C}$  is still visible. The bottom graphs in figure 1(a) and figure 1(b) of the samples annealed at  $1100^\circ\text{C}$  display the only remaining vibration band centred around  $800^\circ\text{C}$  with a superimposed shoulder above  $840 \text{ cm}^{-1}$  wavenumber concomitant with the disappearance of the  $\text{CH}_n$  vibration component above  $960 \text{ cm}^{-1}$ .

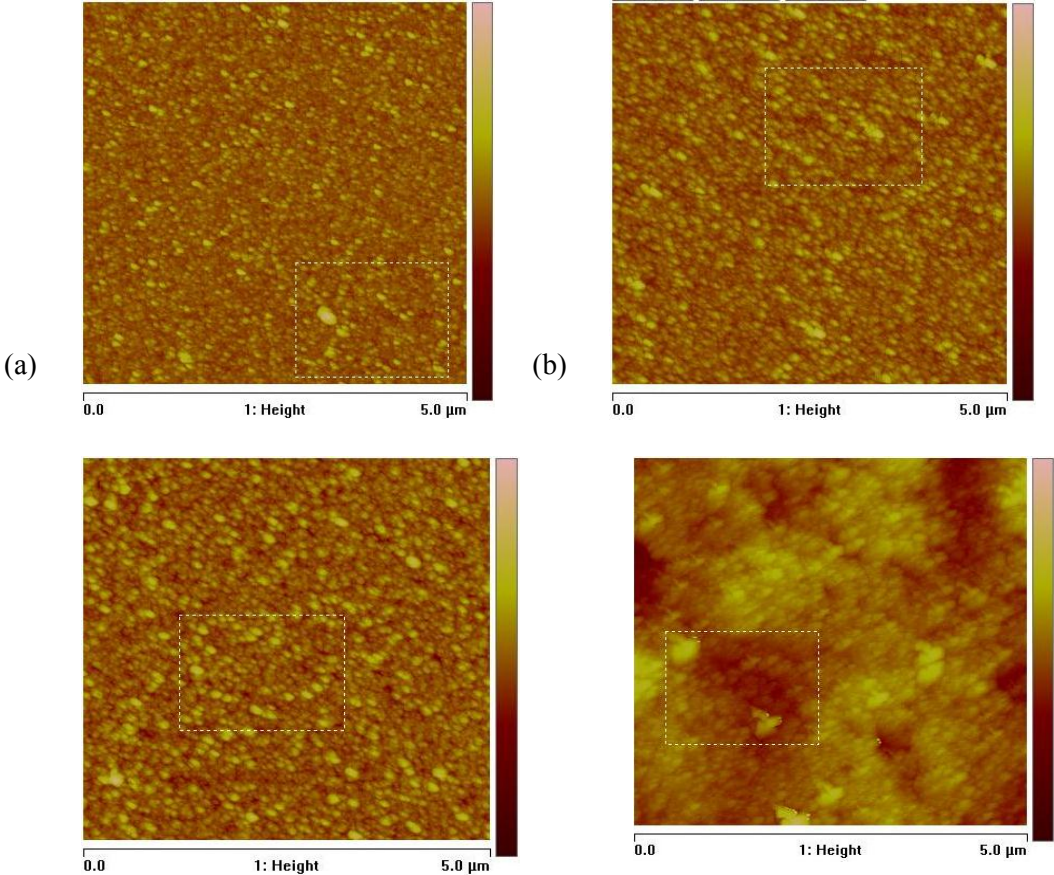
Figure 2 gives the AFM images of the as-deposited films and of those annealed. The images of both as- deposited films show as smooth surface with clear dispersed crystals; these are mainly Si polycrystals (as it has been revealed by the EDX investigation in STEM mode). The AFM images of the samples annealed at  $700^\circ\text{C}$  show distorted elongated grains; at this temperature the cracking of the  $\text{SiH}_n$  and the effusion of the released hydrogen are complete. The images of the samples annealed at  $900^\circ\text{C}$  reveal an increased density of the crystallites with conical shape while at  $1100^\circ\text{C}$  temperature of anneal, the AFM images of both studied samples show a microstructure characterized by a coalescence of the small grains in large clusters. Table 2 gives a summary of the average roughness and grains/clusters diameter calculated from AFM data.

Figure 3(a) displays a typical cross-section TEM image of the films as taken from the as-deposited S<sub>2</sub> sample; a crystalline columnar growth mainly perpendicular to the c-Si substrate is observed. This feature is similar to that obtained in microcrystalline Si ( $\mu\text{-Si:H}$ ) films with high crystalline volume

fraction [12]. The crystalline columns are built from smaller crystalline grains of a few tens of nanometers in size; in low crystalline material the column structure is less developed and individual small features are normally observed [13]. The EDX spectrum profile collected over a line scan in STEM mode of the same sample (see figure 3(b)) shows a much more dominant peak of Si compared to that of C; this result indicates that the observed SiC phase is embedded in a  $\mu\text{-Si:H}$  matrix.



**Figure 1.** FTIR spectra of as- deposited and annealed samples (a) sample S<sub>1</sub> (b) sample S<sub>2</sub>



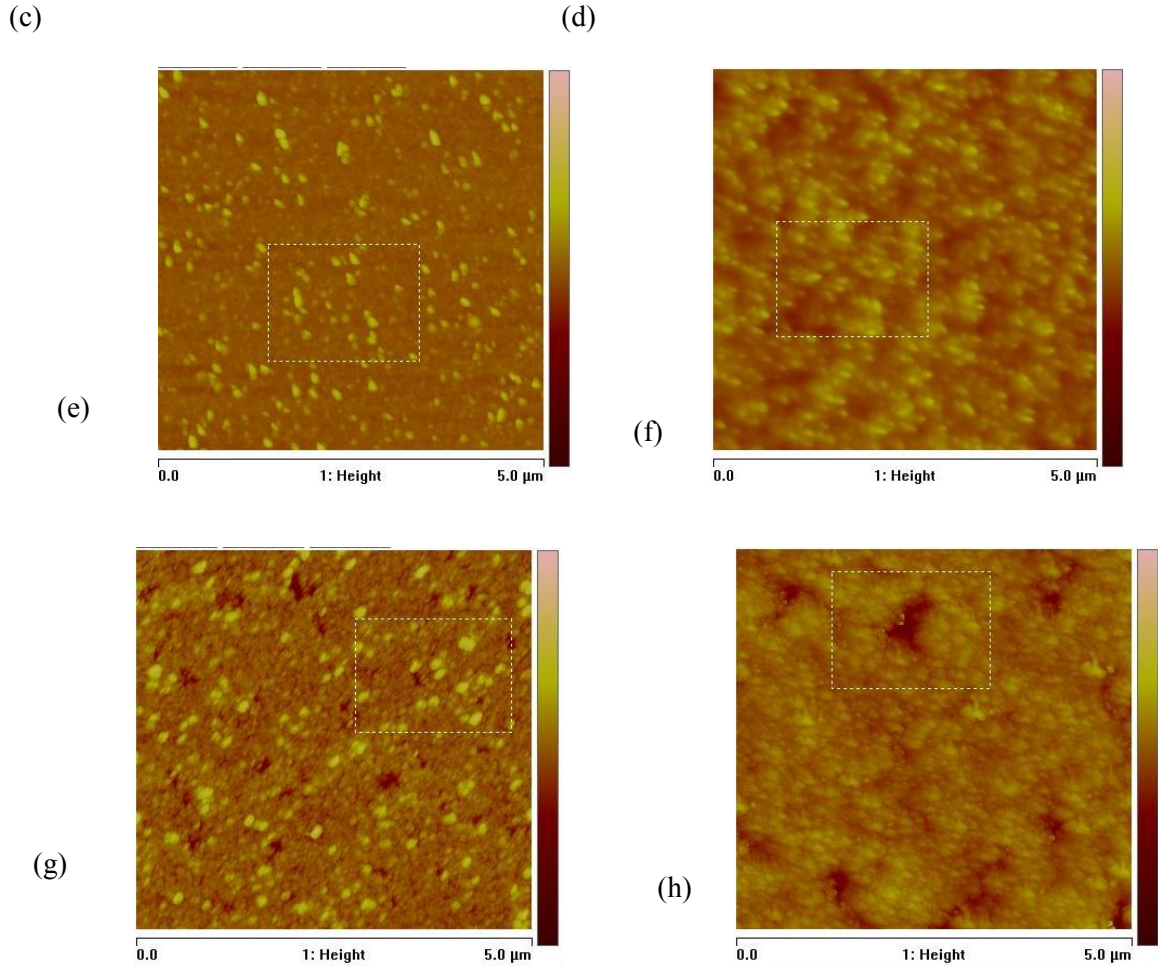


**Figure 2.** AFM images of the samples as-deposited and annealed: (a) S<sub>1</sub> as deposited, (b)-(d) S<sub>1</sub> annealed at 700°C, 900°C and 1100°C respectively; (e) S<sub>2</sub> as deposited, (f)-(h) S<sub>2</sub> annealed at 700°C, 900°C and 1100°C respectively.

**Table 2.** Average roughness and crystals/clusters diameter.

Sample		As-depo	700°C	900°C	1100°C
S1	Roughness (nm)	4.83	5.27	6.19	21.10
	Diameter (μm)	0.15	0.14	0.22	0.34
S2	Roughness (nm)	3.27	4.18	5.64	13.30
	Diameter (μm)	0.14	0.13	0.16	0.30

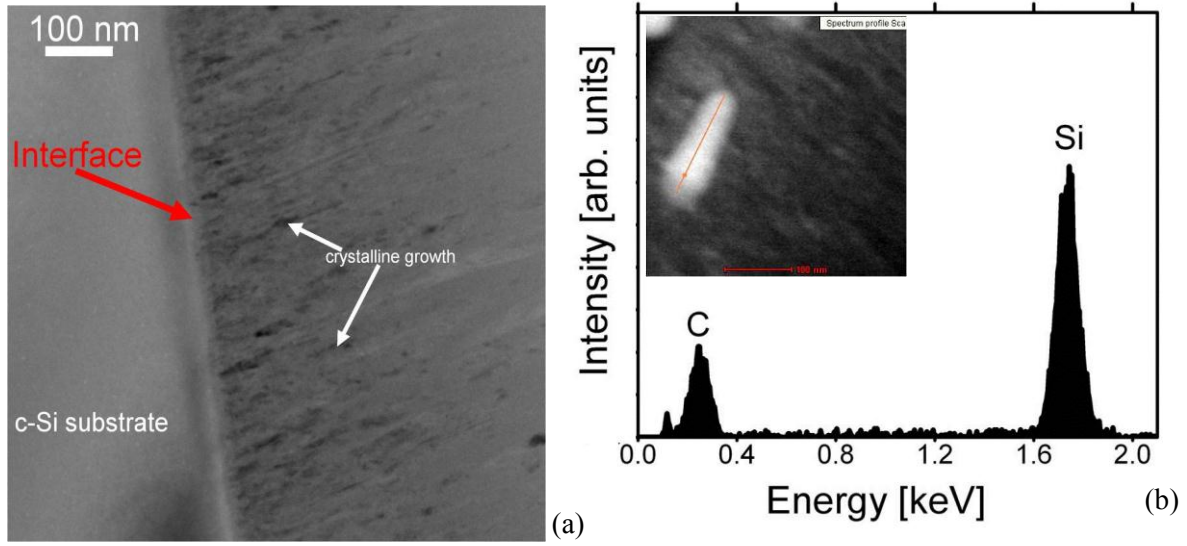


Figure 3. (a) TEM cross-section image of a specimen prepared from sample  $S_2$  as-deposited. (b) EDX spectrum taken at one of the points of the line scan indicated on the STEM micrograph in the insert.

### 3.2. Discussion

The microstructure of thermally induced  $\mu\text{-SiC:H}$  was extensively investigated by FTIR, AFM and TEM. The films are grown either as amorphous ( $S_1$ ) or nanocrystalline  $\text{SiC:H}$  ( $S_2$ ). The annealing treatment of the samples causes first the cracking of the  $\text{Si-H}_n$  molecules whose absorption bands in FTIR are observed to decrease in intensity and vanish at  $700^\circ\text{C}$  annealing temperature. At this stage, following the effusion of hydrogen from the samples, a rearrangement of the network is observed on the AFM image that shows rather distorted crystal grains. On the sample annealed at  $900^\circ\text{C}$ , a quasi-symmetrical absorption band due to crystalline  $\text{SiC}$  phase coexists with a signature of the remaining  $\text{C-H}_n$  bonds around  $1000\text{ cm}^{-1}$ . A much more interesting fact though is observed at the annealing temperature of  $1100^\circ\text{C}$  where a shoulder is appearing on the  $800\text{ cm}^{-1}$   $\text{SiC}$  vibration peak around  $850\text{ cm}^{-1}$  wavenumber while the  $1000\text{ cm}^{-1}$   $\text{CH}_n$  vibration band is simultaneously disappearing. The resultant band is only well fitted by 2 Gaussian peaks centred at  $770\text{ cm}^{-1}$  and  $856\text{ cm}^{-1}$  as well as a Lorentzian centred at  $800\text{ cm}^{-1}$ . While the first Gaussian at  $770\text{ cm}^{-1}$  and the Lorentzian at  $800\text{ cm}^{-1}$  along with another  $\text{SiH}$  related Gaussian peak at  $830\text{ cm}^{-1} - 850\text{ cm}^{-1}$  have been widely reported in as-deposited  $\text{SiC}$  materials [2, 14-15], to our knowledge this broad Gaussian peak observed at high wavenumber in annealed samples has not been reported previously. Given the nature of its wide width, it signifies a broad distribution of  $\text{SiC}$  bond lengths and bond angles in the network. We propose thus that it should be included in the estimation of the  $\text{SiC}$  crystalline volume fraction ( $f_{\text{SiC}}$ ) in the films;  $f_{\text{SiC}}$  should be given by

$$f_{\text{SiC}} = \frac{A_{800}}{A_{770} + A_{800} + A_{856}} \quad (1)$$

where  $A_{770}$ ,  $A_{800}$  and  $A_{856}$  are the areas under the deconvoluted peaks centred at  $770\text{ cm}^{-1}$ ,  $800\text{ cm}^{-1}$  and  $856\text{ cm}^{-1}$  respectively. Applied to the annealed films at  $1100^\circ\text{C}$ , the method returns  $f_{\text{SiC}}$  values equal to 43.8 % and 48.3 % for  $S_1$  and  $S_2$  samples respectively.



#### 4. Conclusion

a-SiC:H and nc-SiC:H have been prepared by the HWCVD process using a SiH<sub>4</sub>/CH<sub>4</sub>/H<sub>2</sub> mixture at low temperature of the substrate. The samples have been subjected to a vacuum annealing up to 1100°C. The structural properties of the films are studied by FTIR, AFM and TEM. It is shown that the SiH<sub>n</sub> related peaks are the first to disappear at the annealing temperature of 700°C while those associated to CH<sub>n</sub> crack completely only above 900°C. The resulting material at the last annealing temperature of 1100 °C shows a unique vibration signature corresponding to crystalline SiC, as detected by FTIR at 800 cm<sup>-1</sup> wavenumber. This peak can be deconvoluted into two broad disorder-related Gaussian components at 770 cm<sup>-1</sup> and 856 cm<sup>-1</sup>, and a narrow Lorentzian peak that signifies the presence of SiC ordered phase.

#### Acknowledgements

The authors wish to thank the National Research Foundation (NRF) for funding the main author's research project, the Chemistry department at UWC and iThemba LABS for FTIR and AFM measurements respectively.

#### References

- [1] Finger F, Astakhov O, Bronger T, Carius R, Chen T, Dasgupta A, Gordijn A, Houben L, Huang Y, Klein S, Luysberg M, Wang H and Xiao L 2009 *Thin Solid Films* **517** 3507
- [2] Chen T, Köhler F, Heidt A, Huang Y, Finger F and Carius R 2011 *Thin Solid Films* **519** 4511
- [3] Miyajima S, Haga K, Yamada A and Konagai M 2006 *Jpn. J. Appl. Phys.* **45** 432
- [4] Kunii T, Honda T, Yoshida N and Nonomura S 2006 *J. Non-Cryst. Solids* **352** 1196
- [5] Halindintwali S, Knoesen D, Swanepoel R, Julies B A, Arendse C, Muller T, Theron C C, Gordijn A, Bronsveld P C P, Rath J K and Schropp R E I 2007 *Thin Solid Films* **515** 8040
- [6] Halindintwali S, Knoesen D, Swanepoel R, Julies B A, Arendse C, Muller T, Theron C C, Gordijn A, Bronsveld P C P, Rath J K and Schropp R E I 2009 *South Afric. J. Sci.* **105** 290
- [7] Lau W S 1999 *Infrared Characterization of Microelectronics* World Scientific (Singapore)
- [8] Zhang S, Pereira L, Hu Z, Ranieiro L, Fortonato E, Ferrira I and Martins R 2006 *J. Non Cryst. Solids* **352** 1410
- [9] Waman V S, Kamble M M, Pramod M R, Gore S P, Funde A M, Hawaldar R R, Amalnerkar D P, Sathe V G, Gosavi S W and Jadkar S R 2011 *J. Non Cryst. Solids* **357** 3616
- [10] Swain B P 2006 *Materials letters* **60** 2767
- [11] Swain P B and Dusane O R 2006 *Materials Chemistry and Physics* **99** 240
- [12] Finger F 2010 *Thin-Film Silicon Solar Cells* EPFL Press (Switzerland) 97-143
- [13] Houben L, Luysberg M, Hapke P, Carius R, Finger F and Wagner H 1998 *Philos. Mag. A* **77** 1447
- [14] Chen T, Yang D R, Carius R and Finger F 2010 *Jpn. J. Appl. Phys.* **49/4**
- [15] Kerdiles S and Rizk R 2002 *Philos. Mag. A Phys. Condens. Matter Struct. Defects Mech. Prop.* **82/3** 601